Permeability of Oxygen and Nitrogen Gases in Ethyl Cellulose Solid Films Retaining Cholesteric Liquid Crystalline Order

SHINICHI SUTO,* TOMOHITO NIIMI, and TERUSADA SUGIURA

Department of Materials Science and Engineering, Faculty of Engineering, Yamagata University, Jonan 4-3-16, Yonezawa, Yamagata 992, Japan

SYNOPSIS

Ethyl cellulose (EC) films that retain lyotropic and thermotropic cholesteric liquid crystalline order, and an amorphous EC film were prepared. The liquid crystalline order was identified by optical measurements. The comparative permeability of oxygen and nitrogen gases for three kinds of EC film was determined, and the applicability of the EC films that retained cholesteric liquid crystalline order to oxygen enrichment are discussed. The permeability of oxygen or nitrogen gas for the liquid crystalline films was lower than that for the amorphous ones. The activation energy for the permeability coefficient of oxygen gas was ca. 3.5 kcal/mol. The ratio of permeability coefficient for oxygen gas to that for nitrogen gas was less than 4. Interestingly, the permselectivity of oxygen and nitrogen gases for the liquid crystalline films was greater than that for the amorphous ones. © 1996 John Wiley & Sons, Inc.

INTRODUCTION

Recently, the gas transport phenomena in polymeric solid films that retain liquid crystalline order (hereafter, liquid crystalline film) or in the liquid crystalline state of the polymer were reported.[1-13] Almost all the liquid crystalline polymers investigated had nematic or smectic characteristics. There are very few data for gas transport in the cholesteric (twisted nematic) polymeric liquid crystals at present.[14,15]

Some groups succeeded in preparing the cellulosic cholesteric liquid crystalline solid films.[16-20] We also prepared the liquid crystalline hydroxypropyl cellulose (HPC)[21-24] and ethyl cellulose (EC)[25,26] films. One of our final objectives is to make clear the applicability of the cholesteric liquid crystalline films to gas or liquid separation. In this article we consider the EC liquid crystalline films for the following reasons: EC has been the subject of research for oxygen enrichment since the 1950s,[27-29] EC forms both lyotropic and thermotropic liquid crystals at given conditions,[30] and EC is generally amorphous and the effect of the crystalline phase on the gas transport can be ignored. Therefore, EC film is a good model for comparison with the gas transport phenomena in liquid crystalline and amorphous films.

When gas transport phenomena are investigated, fundamentally we need to find out the morphological data of the films used and to consider the relation between the transport phenomena and morphology of the films. Accordingly, in the first part of this article the identification of the liquid crystalline order in the films prepared is described as in our previous article.[24] In the following part the permeability of oxygen or nitrogen gas in the films is determined, and the applicability of the EC cholesteric liquid crystalline films to oxygen enrichment is discussed. We prepared an amorphous EC film that serves as a basis for comparison of the gas permeability.

* To whom correspondence should be addressed.

Journal of Applied Polymer Science, Vol. 61, 1621-1630 (1996)
 CCC 0021-8995/96/101621-10

This paper is a sequel to our previous articles on the cellulosic liquid crystalline films.[24,26]

EXPERIMENTAL

Samples

EC (Tokyo Kasei Kogyo Co. Ltd.) was used as received. The weight-average and number-average molecular weights (M_w and M_n) and degree of substitution (DS) of EC are 12.3×10^4, 3.78×10^4, and 2.67, respectively.[31] Before use, EC powder was dried *in vacuo* at 40°C for ca. 24 h. Commercial reagent grade *m*-cresol and benzene (Wako Pure Chemical Ltd.) were used without further purification.

Preparation of Concentrated Solutions

Given amounts of the EC powder and *m*-cresol were mixed in a glass-stoppered flask. The flask was stored in the dark for ca. 3 months. The concentration of solution was 40 wt %. The critical concentration from the biphase to single-phase liquid crystal (Cb) at 20°C was ca. 30 wt % for our EC/*m*-cresol system.[31] Thus, our EC solution in *m*-cresol was a single-phase liquid crystal. EC solution in benzene (10 wt % concentration) was also prepared but the system never formed liquid crystals.[32]

Preparation of Solid Films

EC liquid crystalline films were prepared by two different processes: solvent cast and hot pressing. The former was intended to provide the films retaining lyotropic liquid crystalline order, while the latter was for the films retaining thermotropic liquid crystalline order. Amorphous films cast from the benzene system were also prepared and acted as an arbitrary basis for comparison.

Table I Conditions for Preparing Ethyl Cellulose Films

Solvent	Initial Concn (wt %)	Hot-Press Temp. (°C)	Film Code
Benzene	10	—	EC-I
m-cresol	40	—	EC-II
		180[a]	EC-III

[a] Pressure of 50 kg/cm² for 30 min.

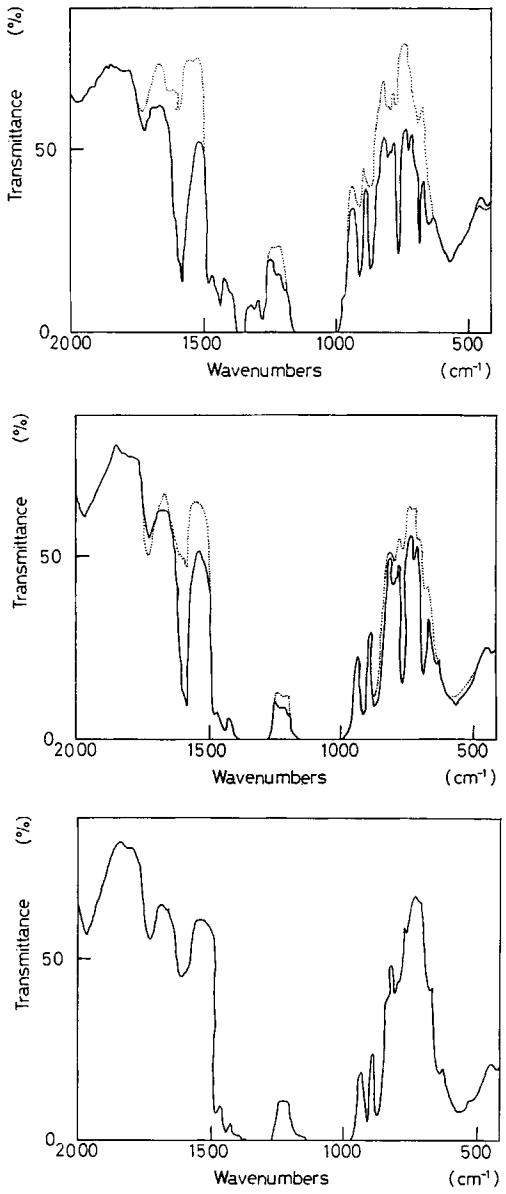

Figure 1 IR spectra for our EC films heat treated at (—) 40°C or (---) 60°C *in vacuo*; (a) EC-I, cast from benzene solution; (b) EC-II, cast from liquid crystalline *m*-cresol solution; and (c) EC-III, hot-pressed at 180°C.

Solvent-Cast Process

A sample solution of ca. 4 g was spreaded slowly with a glass rod (shear rate ca. 54 s^{-1}) on a glass plate framed with 300-μm adhesive tapes parallel to each other on both sides of the plate. The plate was kept over mercury and the solvent was allowed to evaporate for 2–3 weeks in a laboratory atmosphere (ca. 20°C, 65% relative humidity). The resultant film was peeled from the plate, dried *in vacuo* at 40°C

for 3 or 4 days, and then stored in a desiccator over silica gel at room temperature. The thickness of the films was 50–80 μm.

Hot-Pressing Process

Approximately 4 g of the EC powder was placed between two aluminum foils positioned on the platen of a simple hydraulic press. As a spacer, aluminum plates (ca. 50-μm thickness) were placed on four edges of the platen. At 180°C the EC powder was preheated for 2 min, then pressed at 10 kg/cm^2 for ca. 5 min, followed by 50 kg/cm^2 for 30 min. The EC compressed between the aluminum foils was cooled at room temperature. The resultant film was peeled from the aluminum foils and stored in the desiccator. The thickness of the films was 60–100 μm.

The conditions and abbreviations of the resultant films are shown in Table I. Hereafter, each film is denoted by the letter I, II, or III (indicating preparation process).

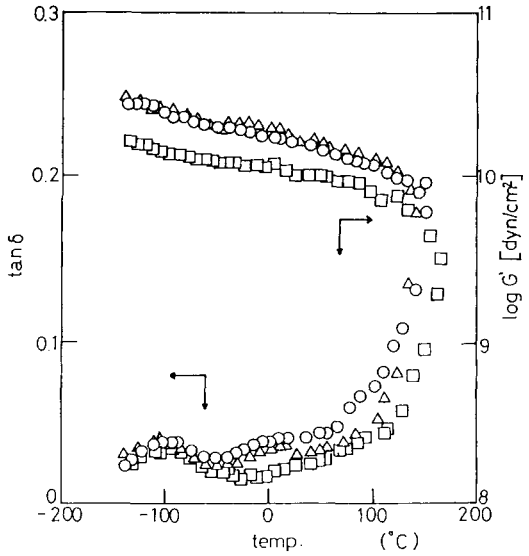

Figure 3 Temperature dependence of dynamic mechanical properties of ethyl cellulose films at 110 Hz; (○) EC-I, (△) EC-II, and (□) EC-III.

Heat Treatment of Cast Films

The films cast from *m*-cresol and benzene systems (EC-II and EC-I) were dried at 40°C *in vacuo*. However, the solvent remained in the cast films. Thermogravimetry (SSC-5200, Seiko, Co. Ltd.) revealed that the residual solvent in each film was 1.5, 3.4, and 0% for the EC-I, EC-II, and EC-III films, respectively. The presence of residual solvent in the cast films was confirmed by infrared spectroscopy (IR-435, Shimadzu Seisakusho Co. Ltd.) at 20°C as shown in Figure 1. The solid line is for the film heated at 40°C and the dotted line is for the film heated at 60°C. Compared with the spectra for the EC-III films, which have no residual solvent, both types of cast film without heat treatment at 60°C exhibited other peaks around 1600 and 720 cm^{-1}, which corresponded to the benzene ring. Therefore, for further removal of the solvent, the cast films were heat treated at 60°C *in vacuo* for 3 days. After heating at 60°C, those peaks of the IR spectrum became weak. The cast films heated at 40°C inevi-

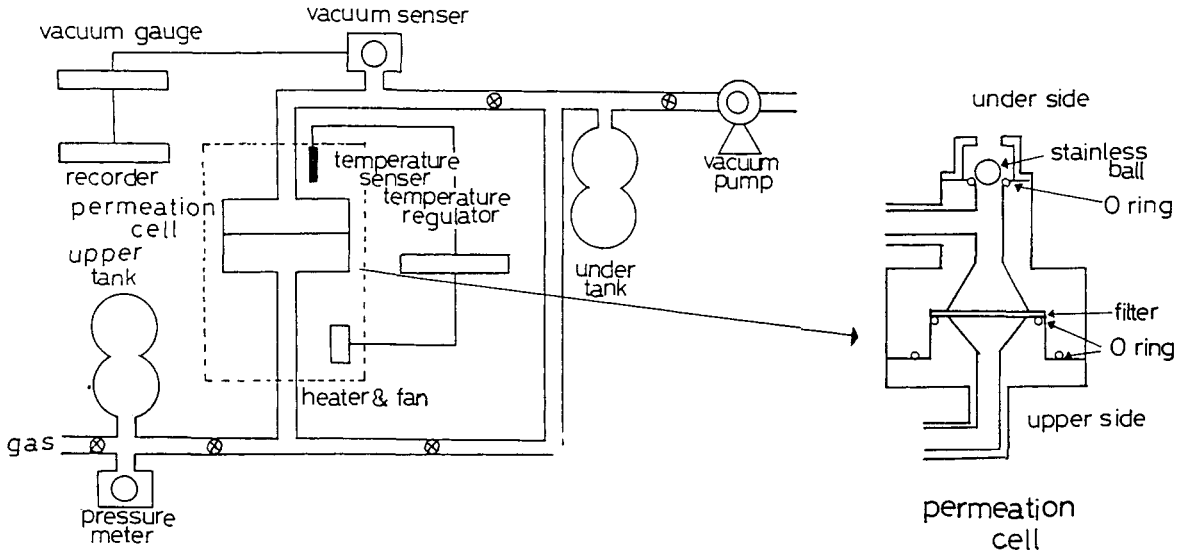

Figure 2 Schematic diagram of our gas permeation apparatus.

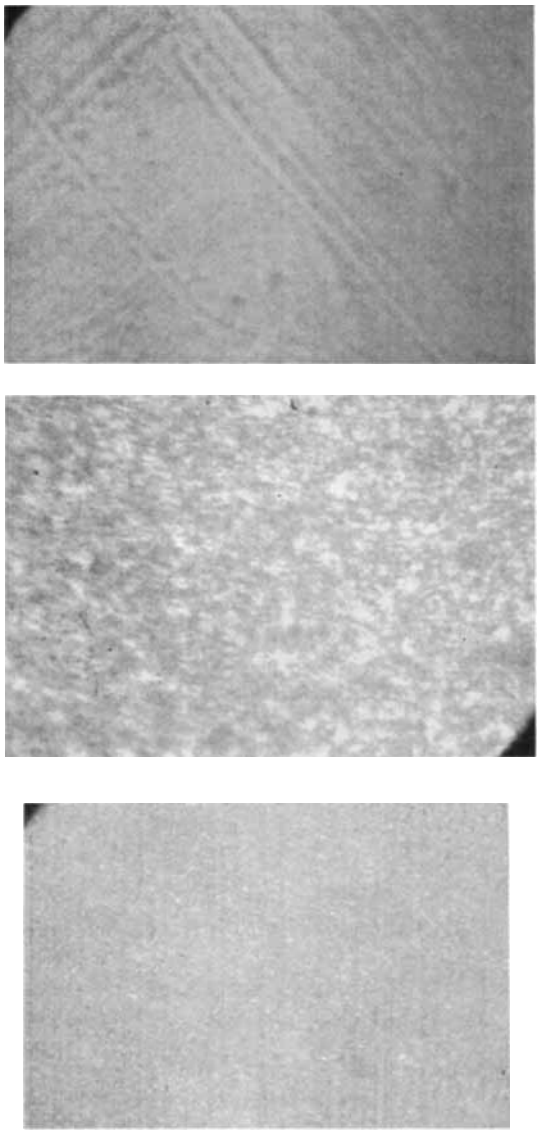

Figure 4 Polarized photomicrographs of the texture for our EC films; (a) EC-I, (b) EC-II, and (c) EC-III.

tably retain the solvent and the further heating at 60°C reduces the amount of residual solvent.

Polarized Microscopical Observation of Films

An Olympus polarized microscope equipped camera was used to observe and photograph the texture of the films under a crossed polarizer with 150× magnification.

Circular Dichroism (CD) of Films

CD spectra of the solid film between glass plates were determined with a Jasco J-40S (Japan Spectroscopic Co. Ltd.) at room temperature in the wavelength range of 200–700 nm.

Scanning Electron Microscopy of Films

The free surface and fractured planes of the films were observed with a scanning electron microscope (S-415, Hitachi Seisakusho, Ltd.). Films were freeze fractured by bending in liquid nitrogen.

Gas Permeability of Films

Gas permeability coefficients were determined by using equipment designed and constructed in our laboratory. The schematic diagram of our gas permeation apparatus is shown in Figure 2. Sample film circularly cut (4-cm diameter) was set in the permeation cell. The cell was thermostated to 20 ± 1°C, unless otherwise noted. The downstream side was vacuumed (ca. 1.35×10^{-5} kg/cm^2). At given pressures at the upstream side (p_1) we determined the pressure at the downstream side (p) as a function of time by means of a vacuum sensor (ULVAC Co. Ltd., WP-02). The time dependence of the pressure suggested that it takes ca. 600 min untill steady state is reached. Consequently, all measurements of the permeation were performed for ca. 2000 min. The gas leak rate in this apparatus was less than 1% in comparison with the gas permeation rate, thus we ignored the gas leak.

The permeability coefficient P is estimated by using eq. (1),

$$P = V \cdot (\Delta p/\Delta t)s \cdot 273/(273 + T) \times 1/76 \cdot l/A \cdot 1/p_1, \quad (1)$$

where V is volume of the downside tank (4299 cm^3), $(\Delta p/\Delta t)s$ is the slope of the steady state, T is temperature, l is film thickness (50–80 μm), and A is the area of the film (4 cm^2).

The gas permeability greatly depends on the experimental temperature that is above or below the glass transition temperature, T_g, of the films.[33] Thus, here we determined the T_g of our films. Figure 3 shows the dynamic mechanical properties of each film, determined with a Rheovibron DDV-II-C (Toyo Baldwin Co. Ltd.). Around 130°C the storage modulus (G') greatly decreased and tan δ increased. This behavior was almost the same as that reported in the literature.[34–36] This indicated that the T_g of our films was ca. 130°C and was almost independent of the preparation process. Our permeation exper-

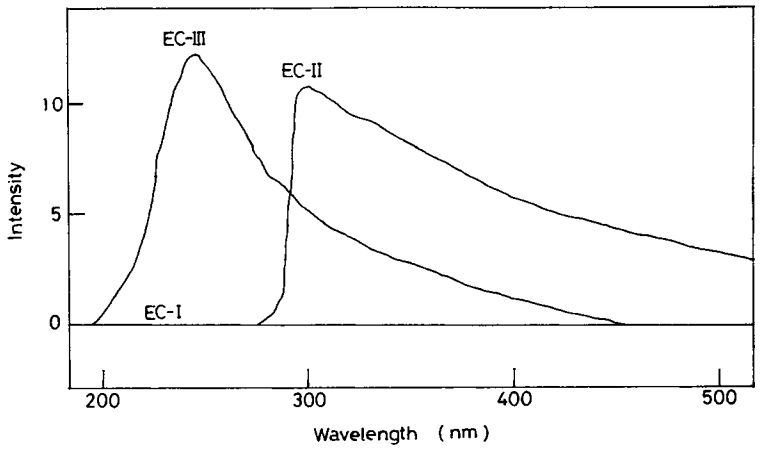

Figure 5 CD spectra for our EC films. The abbreviation of each film is indicated in the figure.

iments were carried out at 20–40°C, meaning that our measurements were carried out at a temperature below the T_g of the EC films. Thus, the permeability coefficient should be estimated on the basis of a partial immobilization model.[33] In our preliminary study, however, we did not adopt the model.

RESULTS AND DISCUSSION

Identification of Liquid Crystalline Order in Films

Figure 4 shows the polarized photomicrographs of the texture for the EC films. The EC-I film exhibited no texture. On the other hand, the EC-II and EC-III films exhibited mosaiclike textures; the texture for the EC-III film was not as clear as that for the EC-II film. The mosaiclike texture was similar to the texture of cellulosic liquid crystalline solutions.[16,37–41]

Figure 5 shows the CD spectra for the EC films. The EC-II and EC-III films exhibited a positive peak at each wavelength, whereas the EC-I film did not peak. This clearly indicated that the *m*-cresol cast film and the hot-pressed film retained the left-handed cholesteric liquid crystalline order and the benzene cast film did not. Generally, the wavelength of the peak of the CD spectrum is related to the cholesteric pitch: the wavelength of the peak is directly proportional to the pitch.[42] Consequently, comparison between CD spectra for the EC-II and EC-III films revealed that the cholesteric pitch for the EC-II film was longer than that for the EC-III film. Figure 6 shows the scanning electron photomicrographs of fractured and free-surface planes for each film. The texture of fractured plane depended on the preparation process: the EC-I film showed a relatively smooth texture, whereas the EC-II and EC-III films showed fluffy textures typically observed for liquid crystals. In the free-surface plane, the EC-I film showed a wrinkle texture, and the EC-II and EC-III films showed a relatively smooth texture.

Our findings noted above clearly indicated that the benzene cast film was amorphous as expected, and the other films (*m*-cresol cast and hot-pressed films) retained the left-handed cholesteric liquid crystalline order. This was the same as that reported in our previous work.[24] Our films seemed to be homogeneously dense. The findings are summarized in Table II.

Cellulosic liquid crystals form polydomain textures.[43] The domain size in our films was not determined, but the size during creep deformation, that is, the Eyring's activated volume V, for our films was determined.[24,26] The value of V appears to be a quick guide to estimating qualitatively the average size of a domain. Therefore, the value of V for each film is also shown in Table II.

Gas Permeability in EC Films

As noted in the Experimental section, our cast films contained the residual solvent, more or less. The permeability coefficient P of the oxygen gas for the cast film (EC-II) heat treated at 40 or 60°C, determined at 35°C, is shown in Figure 7. This indicates that further heat treatment tends to increase P. Compared with P for the heat-treated and hot-pressed films, P for the heat-treated film was lower than that for the hot-pressed one. The difference in

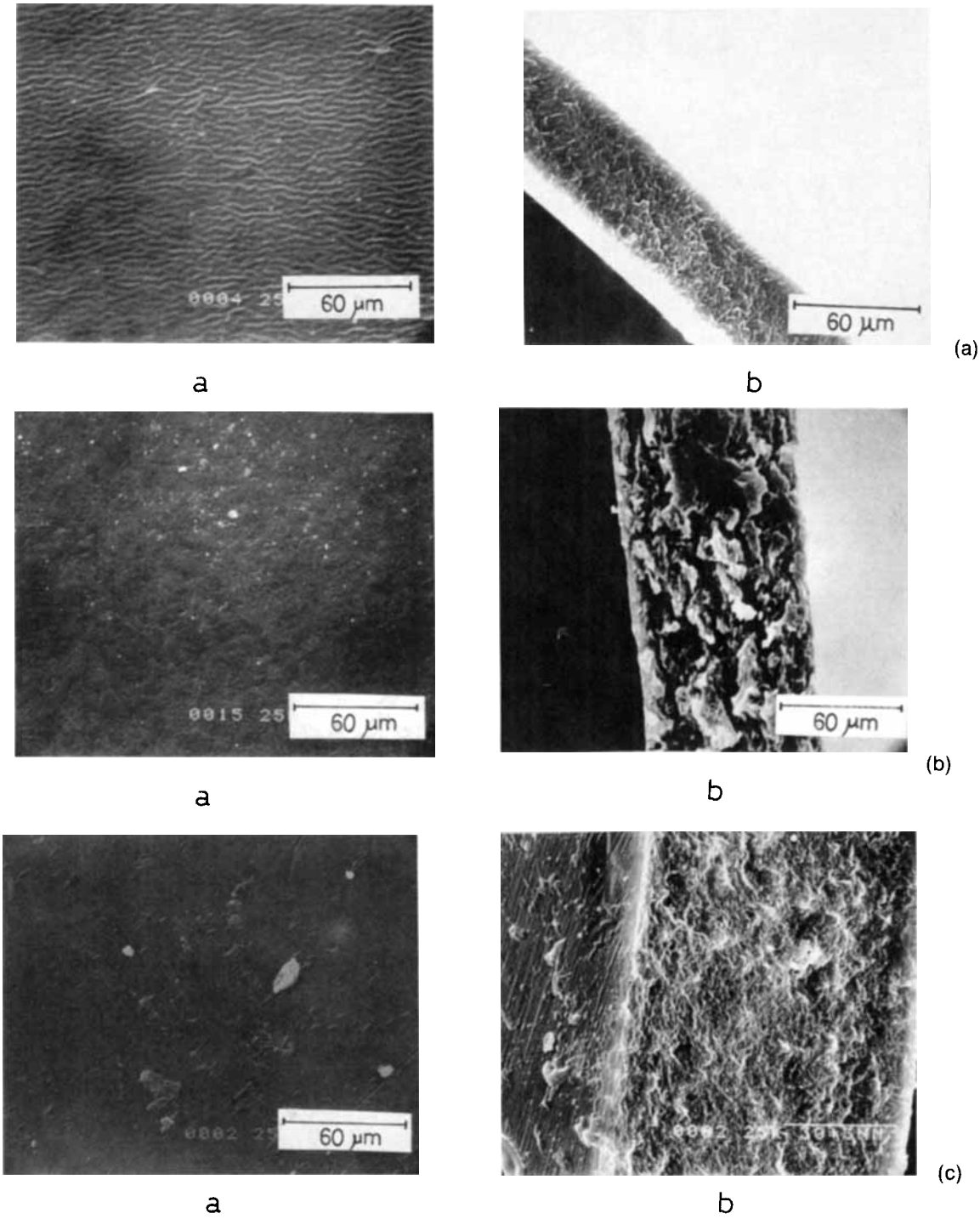

Figure 6 Scanning electron photomicrographs of (a) free-surface and (b) fractured planes for our EC films (original magnification ×500); (a) EC-I, (b) EC-II, and (c) EC-III.

P of the EC-II and EC-III films could be regarded as significant. This suggested that the residual solvent prevents gas diffusion. The CD spectra for the heat-treated films were almost the same as those shown in Figure 5: the cholesteric pitch was independent of heat treatment in our conditions. We suppose that the residual solvent has a minor effect on the gas permeability in our films and the choles-

Table II Morphological Characteristics of Ethyl Cellulose Films

Film Code		Cholesteric Pitch	Domain Size	V^a (nm^3)
EC-I	Amorphous	—	—	1.265
EC-II	Lyotropic liquid crystal	Long	Big	1.226
EC-III	Thermotropic liquid crystal	Short	Small	—

[a] Eyring activated volume at 23°C.

teric liquid crystalline order has a major effect. Consequently, we show the data for the films without heat treatment at 60°C later.

Pressure Dependence

Figure 8 shows the dependence of the nitrogen or oxygen gas permeability coefficient on the upstream side pressure p_1 for the amorphous EC-I film. The order of P for nitrogen gas was ca. 5×10^{-10} and that for oxygen gas was ca. 13×10^{-10}. This order was the same as that reported by Hsieh[29] for the amorphous EC films. With increasing pressure, P decreased, regardless of gas species. P for the EC-II and EC-III films behaved similarly to that for the EC-I film. This was the general behavior for polymeric films below T_g.

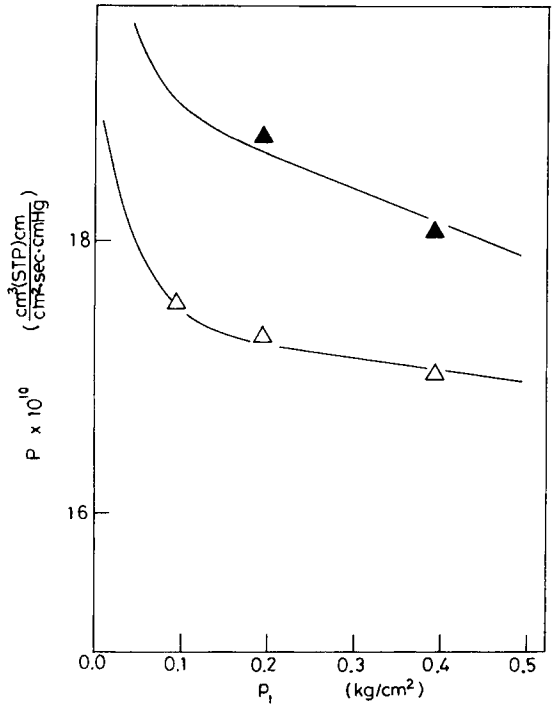

Figure 7 Upper pressure dependence of oxygen gas permeability coefficient at 35°C for EC-II films heat treated at (△) 40°C or (▲) 60°C *in vacuo*.

Effect of Liquid Crystalline Order

Figure 9 shows the nitrogen gas permeability coefficient for three types of film prepared by different processes. P for the EC-I film (amorphous) was greater than that for the EC-II film (lyotropic liquid crystalline) or for the EC-III film (thermotorpic liquid crystalline). The behavior of P may be explained on the basis of molecular packing: the higher the packing of molecules, the lower the permeability. As shown in Table II, the cholesteric pitch for the EC-III film was shorter than that for the EC-II film. This means that the molecular packing for the EC-III film is more dense than that for the EC-II film. Needless to say, the molecular packing for the liquid crystalline state is greater than that for the amorphous state. This was estimated from the values of V shown in Table II.

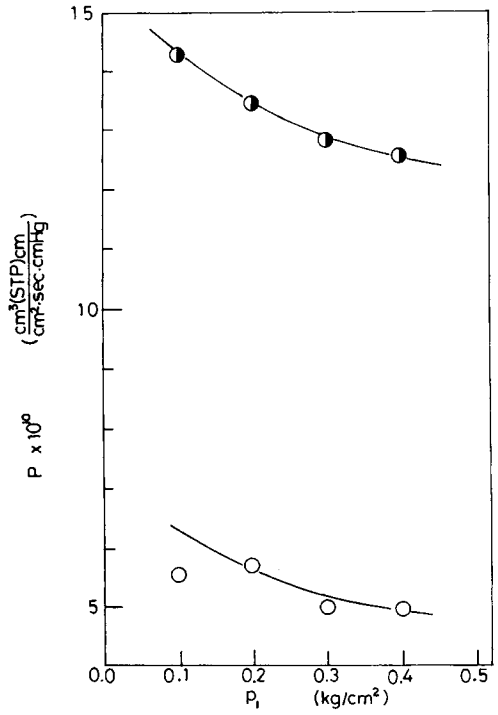

Figure 8 Upper pressure dependence of (○) nitrogen or (◑) oxygen gas permeability coefficient for EC-I film.

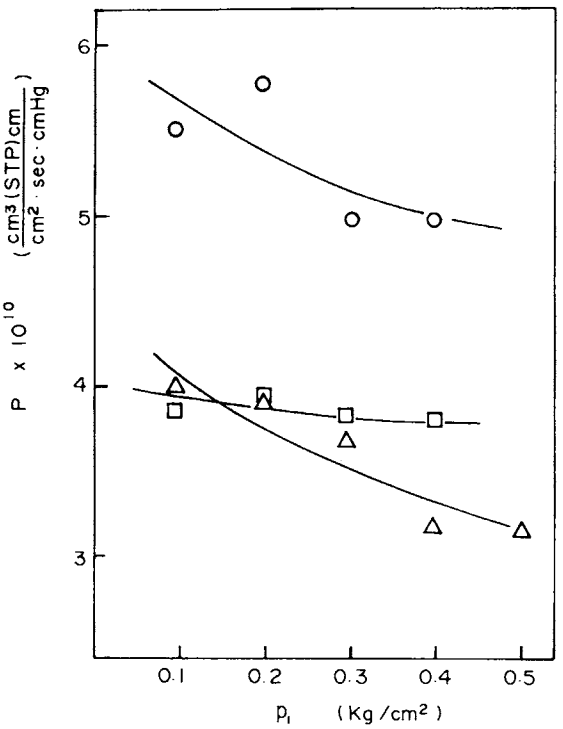

Figure 9 Comparison of nitrogen gas permeability coefficient for (○) EC-I (△) EC-II, and (□) EC-III.

The trend for oxygen gas was the same as that for nitrogen gas, as shown in Figure 10. The principal finding deduced from Figures 9 and 10 was the permeability for the liquid crystalline films was smaller than that for the amorphous ones. It was noteworthy that the difference in values of P between the amorphous and liquid crystalline films, especially between the EC-I and EC-II films, was not as large as expected. This is partially because the liquid crystalline order in our films seemed to be relatively low; the order parameter for our films was less than 0.6.[44] Strictly speaking, we cannot neglect the possibility that the residual solvent plays some role in the gas transport phenomena in our cast films.

For the polymeric liquid crystalline films, it is still unclear whether gases can permeate through a liquid crystalline phase. Weinkauf and Paul[3,4] recently proposed a model that gases transport in the boundary of liquid crystalline domains for thermotropic nematic liquid crystals. However, Vittoria et al.[6] explained the transport phenomena for the side-chain polymeric liquid crystals in terms of a biphasic model that consisted of less-ordered and well-ordered liquid crystalline phases: gases transport through the less-ordered phase. As noted above, we suggested that the gases permeate through a liquid crystalline phase that is not so well-ordered. For cellulosic liquid crystals, molecules are are wormlike not rodlike.[45] Thus, the molecular order of cellulosic liquid crystals is intrinsically less than that of other main-chain liquid crystals. Consequently, it seemed difficult to exclude the following possibility that gases permeate through the cellulosic liquid crystalline phase.

Effect of Temperature on Oxygen Permeability in EC-II Film

P determined at 20, 35, and 45°C increased with temperature. The Arrhenius plots of P were almost linear, as shown in Figure 11, and the activation energy was obtained. The values at given pressures are shown in Table III, where the values are ca. 3.5–3.8 kcal/mol and are a little smaller than that reported for the nematic liquid crystalline film.[1]

Permselectivity of Nitrogen and Oxygen Gases

As shown in Figures 8 and 9, P for oxygen gas was greater that that for nitrogen gas, regardless of types of film. This is mainly due to the difference in the size of the gases: the size of oxygen is 3.46 Å and

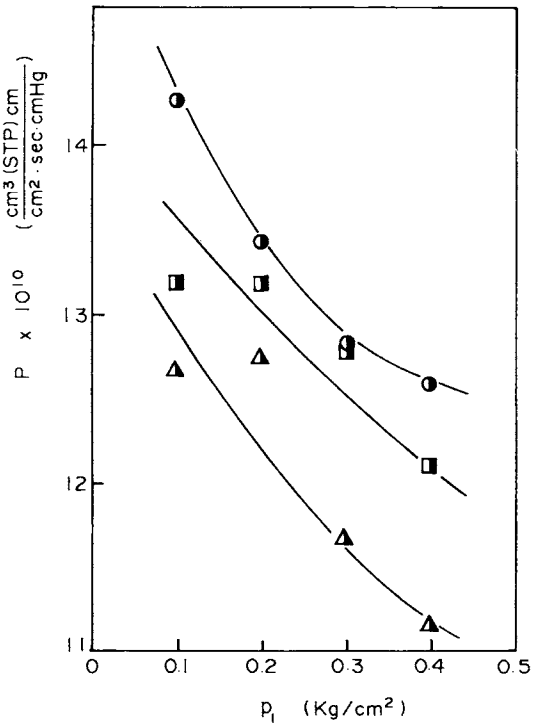

Figure 10 Comparison of oxygen gas permeability coefficient for (◑) EC-I, (▲) EC-II, and (◨) EC-III.

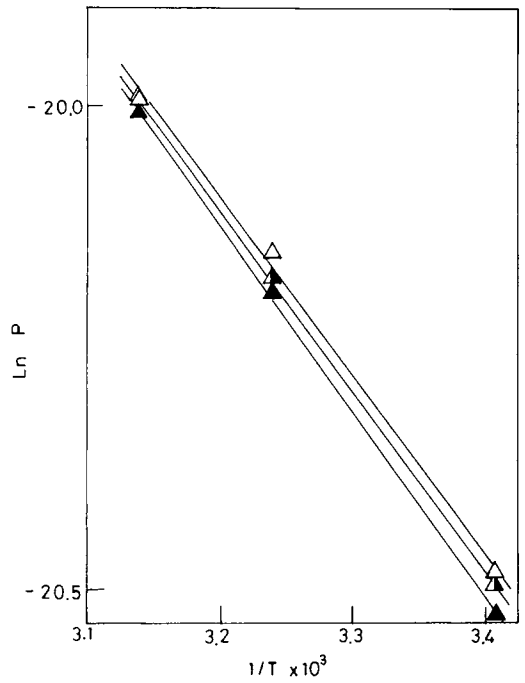

Figure 11 Arrhenius plot of oxygen gas permeability coefficient for EC-II film at given upper pressures (kg/cm^2): (△) 0.1, (▲) 0.2, and (▲) 0.4.

that of nitrogen is 3.64 Å.[46] Here we defined the permselectivity of our EC film to a pair of oxygen and nitrogen gases as the ratio of P for oxygen gas to that for nitrogen gas, $\alpha = P_{ox}/P_{ni}$. The values of α for each film are shown in Table IV. The values were less than 3.54 and were greater than that for the copolypeptides.[15] From an engineering viewpoint, this did not mean the marked applicability of the EC liquid crystalline films to oxygen enrichment. However, it was noteworthy that the values of α for the liquid crystalline films were greater than that for the amorphous ones. This indicated that the cholesteric liquid crystalline film exhibited a better permselectivity than the amorphous ones for a given liquid crystal-forming polymer. Consequently, the cholesteric liquid crystalline texture can possibly improve gas-separation properties.

Table III Activation Energy (E) of Oxygen Gas Permeability at Each Upper Pressure for EC-II Film

Pressure (kg/cm^2)	0.1	0.2	0.4
E (kcal/mol)	3.82	3.76	3.43

Table IV Upper Pressure Dependence of Permselectivity Ratio α for Films

Film Code	Pressure (kg/cm^2) 0.1	0.2	0.3	0.4
EC-I	2.58	2.36	2.56	2.52
EC-II	3.18	3.27	3.27	3.54
EC-III	3.07	3.54	3.28	3.17

We need to prepare the more ordered cholesteric liquid crystalline films and obtain the data on the domain size and the domain boundary to thoroughly understand the transport phenomena in the cellulosic liquid crystalline films.

CONCLUSIONS

Three types of the EC solid film were prepared: the first film cast from benzene solution was amorphous; the second one cast from liquid crystalline solution in *m*-cresol and the third one hot pressed at 180°C retained the left-handed cholesteric liquid crystalline order. The permeability of oxygen or nitrogen gas for the liquid crystalline films was lower that that for the amorphous ones. Effect of temperature on the permeability of oxygen gas for the liquid crystalline film was general and the values of activation energy were smaller than those for other polymeric liquid crystals. The permeability of oxygen gas was greater than that of nitrogen gas for each film. The permselectivity of oxygen and nitrogen was not marked: the ratio of P for oxygen to that for nitrogen α was less than 4. Interestingly, the values of α for the liquid crystalline films were greater than that for the amorphous ones. This suggested that the cholesteric liquid crystalline texture improves the gas separation properties.

The authors gratefully thank Dr. M. Karasawa, Dr. N. Pusch, Mrs. H. Nagasawa, and M. Satoh for help in the design and construction of our gas permeation apparatus.

REFERENCES

1. J. S. Chiou and D. R. Paul, *J. Polym. Sci., Polym. Phys. Ed.*, **25**, 1699 (1987).
2. D. H. Weinkauf and D. R. Paul, *J. Polym. Sci., Polym. Phys. Ed.*, **29**, 329 (1991).

3. D. H. Weinkauf and D. R. Paul, *J. Polym. Sci., Polym. Phys. Ed.*, **30,** 817 (1992).
4. D. H. Weinkauf and D. R. Paul, *J. Polym. Sci., Polym. Phys. Ed.*, **30,** 837 (1992).
5. D. H. Weinkauf, H. D. Kim, and D. R. Paul, *Macromolecules,* **25,** 788 (1992).
6. V. Vittoria, R. Russo, F. D. Candia, P. L. Magagnini, and B. Bresci, *J. Polym. Sci., Polym. Phys. Ed.*, **29,** 1163 (1991).
7. H. Reinecke and H. Finkelmann, *Makromol. Chem.*, **193,** 2945 (1992).
8. D.-S. Chen and G.-H. Hsieu, *Makromol. Chem.*, **194,** 2025 (1993).
9. D.-S. Chen and G.-H. Hsieu, *Polymer,* **35,** 2808 (1994).
10. M. Kajiwara, *J. Mater. Sci.*, **23,** 1360 (1988).
11. T. Hirose, Y. Kamiya, and K. Mizoguchi, *J. Appl. Polym. Sci.*, **38,** 809 (1989).
12. K. Mizoguchi, Y. Kamiya, and T. Hirose, *J. Polym. Sci., Polym. Phys. Ed.*, **29,** 695 (1991).
13. H. R. Allcock, C. J. Nelson, W. D. Coggio, I. Manners, W. J. Koros, D. R. B. Walker, and L. A. Pessan, *Macromolecules,* **26,** 1493 (1993).
14. X.-G. Li, M.-R. Huang, G. Lin, and P.-C. Yong, *J. Appl. Polym. Sci.*, **51,** 743 (1994).
15. Y. Tsujita, R. Ojika, A. Takizawa, and T. Kinoshita, *J. Polym. Sci., Polym. Phys. Ed.*, **28,** 1341 (1990).
16. J. Takahashi, K. Shibata, S. Nomura, and M. Kurokawa, *Sen-i Gakkaishi,* **38,** T-375 (1982).
17. Y. Nishio, T. Yamane, and T. Takahashi, *J. Polym. Sci., Polym. Phys. Ed.*, **23,** 1053 (1985).
18. T. Kyu, P. Mukherjee, and H.-S. Park, *Macromolecules,* **18,** 2331 (1985).
19. G. Charlet and D. G. Gray, *Macromolecules,* **20,** 33 (1987).
20. J. Giasson, J.-F. Revol, A. M. Ritcey, and D. G. Gray, *Biopolymers,* **27,** 1999 (1988).
21. S. Suto, *Kobunshi Ronbunshu,* **40,** 513 (1983).
22. S. Suto, M. Kudo, and M. Karasawa, *J. Appl. Polym. Sci.*, **31,** 1327 (1986).
23. S. Suto, T. Iwaya, and M. Karasawa, *Sen-i Gakkaishi,* **45,** 135 (1989).
24. S. Suto, T. Iwaya, Y. Ohno, and M. Karasawa, *J. Mater. Sci.*, **26,** 3073 (1991).
25. S. Suto, K. Oikawa, and M. Karasawa, *Polym. Commun.*, **27,** 262 (1986).
26. S. Suto, K. Oikawa, T. Iwaya, and M. Karasawa, *J. Mater. Sci.*, **26,** 3899 (1991).
27. S. Weller and W. A. Steiner, *J. Appl. Phys.*, **21,** 279 (1950).
28. (a) R. M. Barrer, J. A. Barrie, and J. Slater, *J. Polym. Sci.*, **23,** 315 (1957); (b) R. M. Barrer and J. A. Barrie, *J. Polym. Sci.*, **23,** 331 (1957); (c) R. M. Barrer, J. A. Barrie, and J. Slater, *J. Polym. Sci.*, **27,** 177 (1958).
29. P. Y. Hsieh, *J. Appl. Polym. Sci.*, **7,** 1743 (1963).
30. S. Suto, J. L. White, and J. F. Fellers, *Rheol. Acta,* **21,** 62 (1982).
31. S. Suto, M. Ohshiro, W. Nishibori, H. Tomita, and M. Karasawa, *J. Appl. Polym. Sci.*, **35,** 407 (1988).
32. D. G. Gray, *J. Appl. Polym. Sci., Appl. Polym. Symp.*, **37,** 179 (1983).
33. D. R. Paul, *Ber. Bunsenges. Phys. Chem.*, **83,** 294 (1979).
34. A. H. Chan, W. J. Koros, and D. R. Paul, *J. Membr. Sci.*, **3,** 117 (1978).
35. P. Sakellariou, R. C. Rowe, and E. F. T. White, *Int. J. Pharmacol.*, **27,** 267 (1985).
36. J.-Y. Wang and G. Charlet, *Macromolecules,* **26,** 2413 (1993).
37. J. Bheda, J. F. Fellers, and J. L. White, *Colloid Polym. Sci.*, **258,** 1335 (1980).
38. Y. Onogi, J. L. White, and J. F. Fellers, *J. Polym. Sci., Polym. Phys. Ed.*, **18,** 663 (1980).
39. G. H. Meeten and P. Navard, *J. Polym. Sci., Polym. Phys. Ed.*, **26,** 413 (1988).
40. M. Horio, E. Kamei, and K. Matsunobu, *Nihon Reoroji Gakkaishi,* **16,** 27 (1988).
41. M. Fujiyama, *J. Appl. Polym. Sci.*, **40,** 67 (1990).
42. H. de Vries, *Acta Crystallogr.*, **4,** 219 (1951).
43. T. Asada, H. Muramatsu, R. Watanabe, and S. Onogi, *Macromolecules,* **13,** 867 (1980).
44. S. Suto, S. Kimura, and M. Karasawa, *J. Appl. Polym. Sci.*, **33,** 3019 (1987).
45. R. S. Werbowyj and D. G. Gray, *Macromolecules,* **13,** 69 (1980).
46. R. T. Chern and N. F. Brown, *Macromolecules,* **23,** 2370 (1990).

Received November 7, 1995
Accepted February 13, 1996